4D-STEM phase and orientation analysis of lithium-ion battery anode materials

Introduction

$LiTi_2(PO_4)_3$ is a promising anode material with rhombohedral NASICON structure for solid state phosphate batteries as it is isostructural to the highly conductive solid electrolyte $Li_{1.3}Al_{0.3}Ti_{1.7}(PO_4)_3$ and also matches its electrochemical stability window [1, 2]. It has been shown that particles with spindle-like morphology synthesized by solvothermal reactions are formed from small sub-particles, and contribute to enhanced battery cycling performance compared to sol-gel synthesized material [3]. There is significant interest in research into how microstructural engineering improves the cycling behavior, and to what extent synthesis conditions can be tuned to produce desired morphologies.

Previous microstructural analysis of such $LiTi_2(PO_4)_3$ spindle like particles revealed the presence of two minor secondary phases, identified as TiO_2 nanoparticles and a $LiTiOPO_4$ phase. FIB-SEM tomography revealed the majority of the TiO_2 nanoparticles are connected in a three-dimensional network and there is interest in understanding whether these networks show some level of crystallographic ordering [4]. Due to the fine polycrystalline nature of these networks, conventional phase analysis with TEM selected area diffraction or high-resolution imaging, is not practical and, additionally, the presence of titanium in both phases complicates robust identification of grains with EDX analysis.

A precession-assisted, analytical 4D-STEM, such as TESCAN TENSOR, provides a solution for nanoscale phase and orientation mapping using both electron diffraction and elemental chemistry data, allowing for the visualisation of phase separations and crystallographic ordering. With TESCAN TENSOR, it is possible to map phases and crystal orientations across a user defined field of view, with spatial resolutions down to a few nanometers.

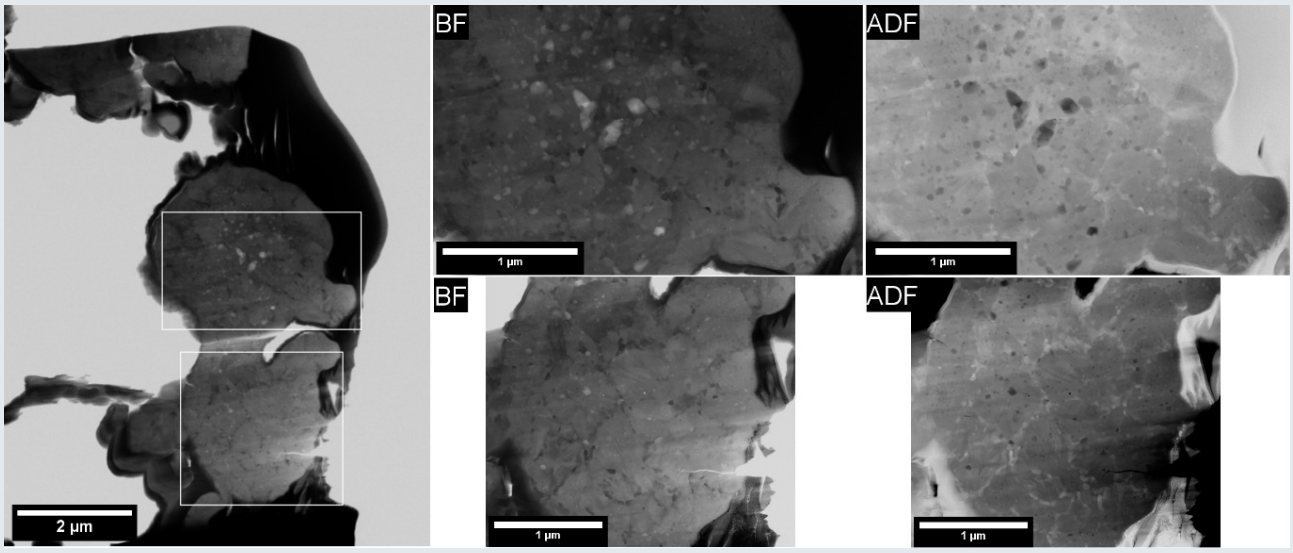

▲ **Figure 1:** Overview BF-STEM images of the specimen, along with BF and ADF-STEM images of regions of interest identified for further analysis

Methods

A lamella was prepared from a synthesised particles using a TESCAN SOLARIS Ga^+ FIB/SEM. From this specimen, STEM images were acquired with a 10 mrad probe convergence semi-angle, a 65 pA probe current, and a pixel dwell time of 3 µs. The ADF detector inner collection semi-angle was set to 15 mrad for diffraction contrast imaging. EDX maps were collected using a 10 nA beam current and 5-minute live time. Orientation and phase analysis was performed using a 2 mrad probe convergence semi-angle, a 50 pA probe current, 14 mrad precession angle, a 1.5 ms pixel dwell time (667 frames per second), and a pixel size of 4.5 nm. Kinematic diffraction templates were generated for known structures of TiO_2 (anatase), $LiTi_2(PO_4)_3$, and $LiTiOPO_4$.

Results and Discussion

STEM-ADF imaging of the FIB prepared specimen showed two distinct regions suitable for analysis (Fig. 1). Both regions are expected to be multiphase, and showed some phase segregation based on local differences in the ADF-STEM image contrast, though this alone was not conclusive proof of phase separations.

The EDX maps in figure 2 showed that whilst it was possible to observe regions with higher titanium and lower phosphorous concentration, it was not possible to directly identify the phases that cause this fluctuation in titanium and phosphorous concentration, though they correlated well with previous research suggesting they were TiO_2.

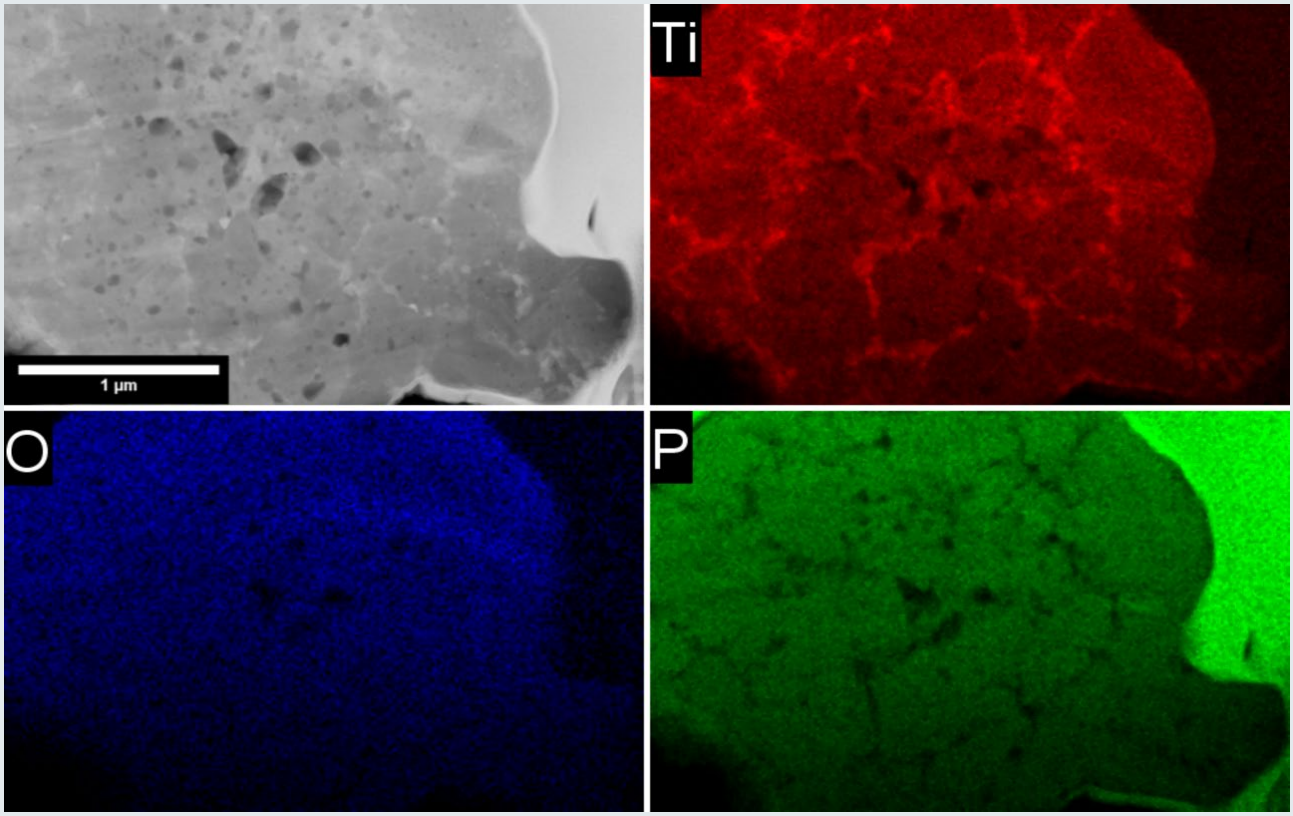

▲ **Figure 2:** ADF-STEM image and corresponding EDX maps taken from the upper region of interest indicated in Fig. 1.

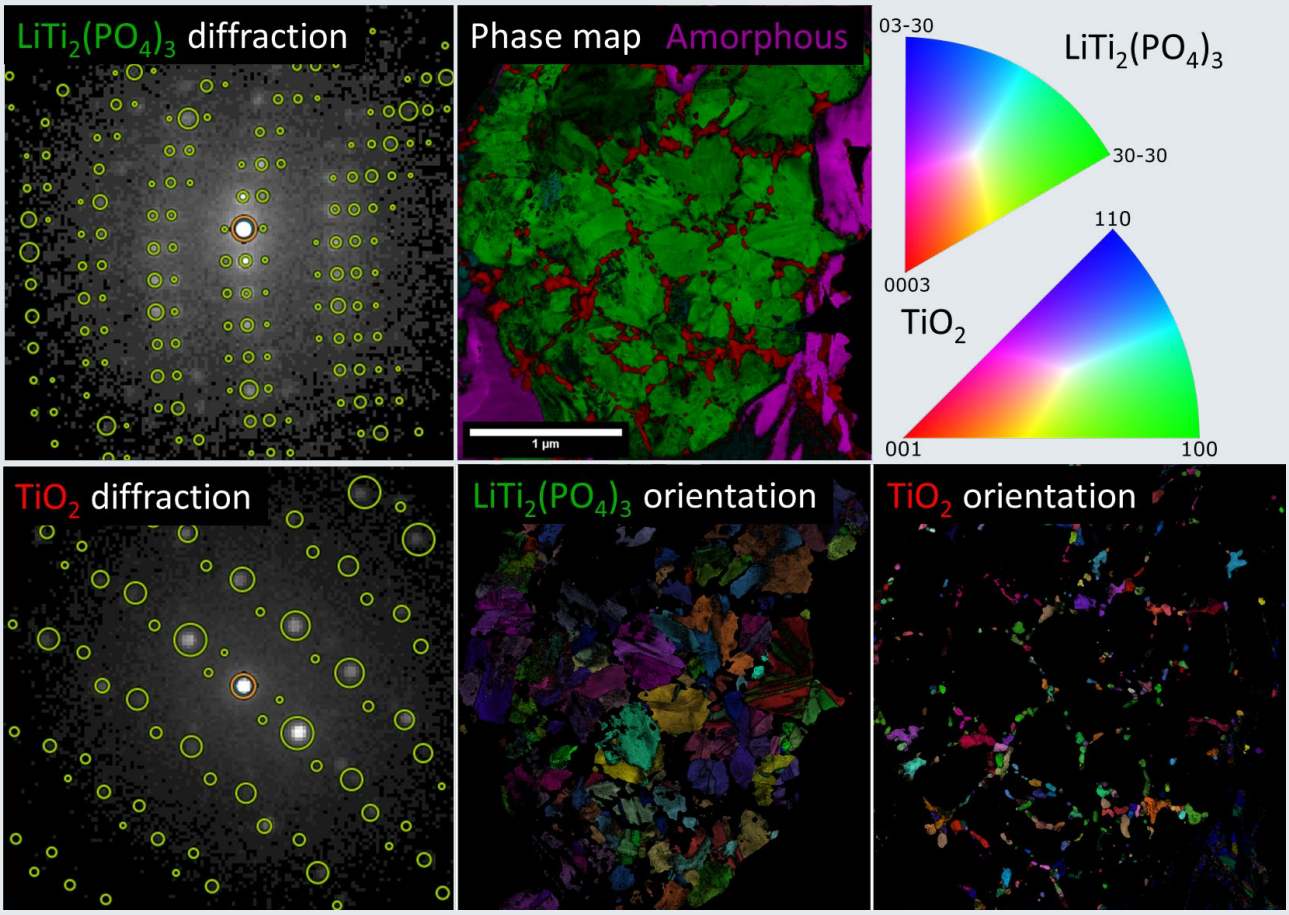

▲ **Figure 3:** Precession assisted 4D-STEM phase and orientation maps for the $LiTi_2(PO_4)_3$ (Green), TiO_2 (Red) with their respective orientation legends. The $LiTiOPO_4$ minority phase is shown in cyan (highlighted in circles), but is not of interest for orientation studies. Example indexed diffraction patterns from each phase are shown.

The titanium rich regions correlated to brighter regions in the ADF image, which suggests they were crystalline and may be measured by electron diffraction based phase analysis, rather than inferred from elemental chemistry data from EDX analysis.

When comparing elemental distribution acquired by EDX to precession-assisted 4D-STEM, the 4D-STEM phase map more clearly shows the differentiation and distribution of known phases (Fig. 3), whereas elemental maps lack this level of differentiation, even when using a large probe current and long acquisition time. This is due to the presence of titanium in all phases, which complicates the differentiation of titanium-bearing phosphates without more advanced post-processing of the data.

The 4D-STEM data provides more conclusive phase analysis when compared to elemental maps, revealing the distribution of the crystallographically differentiated phases, and their relative orientations. The combination of both orientation and phase maps, individually displayed in Figure 3 revealed that the TiO_2 particles were located at the $LiTi_2(PO_4)_3$ sub-particle boundaries. Understanding the grain boundary behaviour and properties of these phases is of significant interest for future research, as these internal sub-particle boundaries can enhance lithium ionic conductivity, improving battery performace.

The phase map in Figure 3, in combination with the $LiTi_2(PO_4)_3$ orientation map, shows the presence of TiO_2 nanoparticles at some $LiTi_2(PO_4)_3$ grain boundaries.

LiTiOPO4 was found to be only a minority phase, detected in two small discrete regions, as such it's relative orientation was not of interest. However, these TiO_2 particles were not observed at all grain boundaries. The network of TiO_2 nanoparticles and sub-particle boundaries may enhance the lithium diffusion inside the $LiTi_2(PO_4)_3$ particles, improving the charge/discharge process, as the ionic conductivity of $LiTi_2(PO_4)_3$ is relatively low. It is observed that whilst there was no strong specimen-wide preferred orientation present, some clusters of the TiO_2 nanoparticles displayed localized preferential orientations, with multiple adjacent particles showing the same orientation. This ordering did not extend through the specimen, it instead remained relatively localised.

Conclusions

Precession assisted 4D-STEM was used to produce maps of $LiTi_2(PO_4)_3$, TiO_2 and small amounts of LiTiOPO4 phases present in spindle-like battery anode particles. 4D-STEM phase analysis shows that TiO_2 nanoparticles form a network at the $LiTi_2(PO_4)_3$ sub-particle boundaries, which may provide a more effective diffusion pathway for lithium ions at higher cycling rates. The $LiTiOPO_4$ was a minority phase detected only in two small regions. Future research into this material system may benefit from precession assisted, analytical 4D-STEM for phase and orientation analysis of phosphates and oxide particles. to investigate the influence of grain orientation and sub-grain phase distributions on the properties of lithium-ion batteries.

References:

[1] Yu, S et al, ACS applied materials & interfaces 10(26), 22264 - 22277 (2018)
[2] Yu, S et al, Journal of the Electrochemical Society 164(2), A370-A379 (2017)
[3] Yu, S et al, ChemElectroChem 3(7), 1157-1169 (2016)
[4] Zhang, Q et al, RSC Advances 11(55), 34605 - 34612 (2021)

TESCAN ORSAY HOLDING, a. s.
Libušina tř. 21, 623 00 Brno - Kohoutovice / Czech Republic
(phone) +420 530 353 411 / (email) sales@tescan.com / marketing@tescan.com